2021

Latent Heat Energy Storage in a Household Refrigerator Powered by Photovoltaic Electricity – Heat Transfer Design and Technical Viability

Carolina Mira-Hernandez
Universidad Pontificia Bolivariana, Colombia, carolina.mira@upb.edu.co

Cesar A. Isaza-Roldan

Latent Heat Energy Storage in a Household Refrigerator Powered by Photovoltaic Electricity – Heat Transfer Design and Technical Viability

Carolina MIRA-HERNÁNDEZ[1]*, César A. ISAZA-ROLDÁN[2]

[1]Universidad Pontificia Bolivariana, School of Engineering
Medellín, Antioquia, Colombia
carolina.mira@upb.edu.co

[2] Universidad Pontificia Bolivariana, School of Engineering,
Medellín, Antioquia, Colombia
cesar.isaza@upb.edu.co

* Corresponding Author

ABSTRACT

In remote rural areas without access to the electrical grid, the use of a stand-alone photovoltaic (PV) installation to drive a domestic refrigerator can be a viable option for adequate food preservation. In this application, energy storage, probably in electric batteries, is required to guarantee refrigeration conditions during periods without solar energy availability. However, electric batteries are still costly, have limited lifespan and use materials with restricted availability. Latent heat thermal energy storage (LHTES) can be an alternative to electric batteries with reduced cost and lower environmental impact. The current study presents general design guidelines for a system with a household refrigerator driven by PV power and with LHTES units. The LHTES units consist of finned panels filled with phase change material (PCM) that are placed on the vertical walls of the compartments, and are passively discharged by free convection. A thermodynamic model is used to size the system components and assess the technical viability of the proposed configuration. Special attention is paid to the heat transfer considerations involved in the design of the LHTES units to guarantee the required charge and discharge powers. The analysis is applied to a 400 L sample commercial refrigerator operating in Medellín, Colombia. It is concluded that the refrigerator necessitates moderate modifications to achieve the technical viability of the proposed configuration.

1. INTRODUCTION

Global warming concerns are accelerating the adoption and development of renewable energy technologies. In recent years, the cost of solar photovoltaic panels has reduced drastically, and the total installed capacity has increased exponentially. In this context, the use of photovoltaic (PV) power to drive domestic refrigerators can be both environmentally beneficial and cost-effective given the significant contribution of domestic refrigerators to household electricity consumption. Moreover, solar PV can be the most affordable alternative for electricity supply in remote rural areas without access to the electrical grid. Life and economic conditions of inhabitants of remote rural areas can be significantly improved by the possibility of refrigerating food and crops.

Solar energy availability is limited to some hours per day. On the other hand, refrigerated conditions of storage compartments are required uninterruptedly to guarantee food preservation. Hence, energy storage is required to compensate the temporal mismatch between solar energy availability and refrigeration demand. However, energy storage poses additional environmental and economic challenges (Tarascon, 2010). In a domestic stand-alone PV installation, electric batteries are the largest contributors to the initial cost. Additionally, electric batteries have a limited lifespan and require special measurements for their final disposal. In household refrigerators driven by PV electricity, the use of cold-thermal energy storage appears as a promising alternative to electric energy storage in batteries. In this application, cold-thermal energy storage can have lower cost and reduced environmental impact.

Latent heat thermal energy storage (LHTES) using phase change materials (PCM) is advantageous because of the high energy storage density that can be achieved compared to sensible heat energy storage (Hasnain, 1998). In addition, LHTES offer an almost constant temperature during charge and discharge (Hasnain, 1998). For a given application, the PCM must have adequate thermo-physical properties, and the LHTES system should be carefully designed to fulfill the temperature and energy storage requirements. The low thermal conductivity of most PCMs can be a major challenge in the development of LHTES systems (E. Oró, de Gracia, Castell, Farid, & Cabeza, 2012). Adequate design of the PCM container can help to overcome the limitations in thermal conductivity (Khodadadi, Fan, & Babaei, 2013). Alternatively, dispersed fillers of highly conductive materials can be added to the PCMs (Kibria, Anisur, Mahfuz, Saidur, & Metselaar, 2015).

Incorporation of PCMs to household refrigerators has been explored as an alternative to improve energy efficiency (Mastani Joybari, Haghighat, Moffat, & Sra, 2015). Different configurations have been assessed, in which the PCM is located either at the evaporator, the condenser or the compartments (Mastani Joybari et al., 2015). Placing the PCM in the refrigerated compartments provides the added benefits of attenuating temperature fluctuations and restraining the temperature rise during periods without electricity availability (B. Gin, Farid, & Bansal, 2010; Mastani Joybari et al., 2015; Eduard Oró, Miró, Farid, & Cabeza, 2012). Usually, the PCM is placed in the refrigerated compartment in planar panels with a volume capacity corresponding to the required energy storage capacity (B. Gin et al., 2010; Benjamin Gin, Farid, & Bansal, 2011; Eduard Oró et al., 2012; Taneja, Lutz, & Culler, 2013). However, the heat transfer design of the panels to comply with specific charge and discharge powers is often overlooked.

Some studies have evaluated the performance of solar-driven refrigerators with LHTES. The studies have mainly focused on experimentally demonstrating the proposed concept for small refrigerators (El-Bahloul, Ali, & Ookawara, 2015; Ewert, Foster, & Estrada, 2001). Also, systems with a similar configuration have been considered for storage of medicines and vaccines (Kouassi, Touré, & Fassinou, 2020).

The current study uses a thermodynamic model to assess the technical viability of a household refrigerator driven by PV electricity and with LHTES units. During periods without solar energy availability, the LHTES units guarantee refrigeration conditions in the compartments without the use of back-up storage in electric batteries. Special attention is paid to the heat transfer aspects of the LHTES units to fulfill the energy absorption and dissipation requirements. The proposed approach is applied to a 400 L commercial frost-free household refrigerator operating in Medellín, Colombia. The requirements for the PV array and the necessary modifications to the refrigerator are discussed.

2. THERMODYNAMIC MODEL AND SYSTEM SIZING

Figure 1 schematically illustrates the energy flows for the household refrigerator driven by PV power and with LHTES. A thermodynamic model is proposed for the household refrigerator in order to determine parameters for the LHTES units and the PV array such as: charge and discharge power, storage capacity, storage density, and solar collection area. The model considers four main components: the refrigerator compartments, the LHTES units, the refrigeration loop, and the PV array. The refrigerator has two compartments, one for frozen-food storage and another one for fresh-food storage. The compartments exchange heat with the environment, the LHTES units, the refrigeration loop, and between them. The objective of the present study is to perform a preliminary evaluation of the technical viability of the proposed system. Hence, only heat gains to the compartments without user interactions are considered. Compartment heat gains are the major drivers of energy consumption in household refrigerators.

A LHTES unit is installed inside each compartment, which consists of panels filled with a PCM of appropriate melting temperature according to the specific compartment temperature range. In Figure 1, the LHTES units are schematically illustrated as being outside of the compartments for the sake of clarity in the formulation of energy balance equations, although they are physically inside the compartments. During periods with sufficient solar energy availability, the power generated by the PV array is used to operate the refrigeration loop and the fans in the compartments. The fans are required to drive air circulation across the evaporator and to actively charge the LHTES units. During periods without sufficient energy availability, the compartments are kept at adequate temperatures by discharging the LHTES units without any power consumption.

For the proposed stand-alone application, the system operates in two distinct modes: charge and discharge. During charge (Figure 1), the LHTES dissipate heat into the compartments and air is actively circulated inside the compartments. The temperature of each compartment must be lowered below the melting temperature of the PCM. During discharge, the LHTES units absorb heat from the compartments, and the temperature in each compartment rises above the melting temperature of the PCM. For design and sizing purposes, a constant temperature of the compartments is assumed for each operating mode. The ambient temperature is also assumed to be constant.

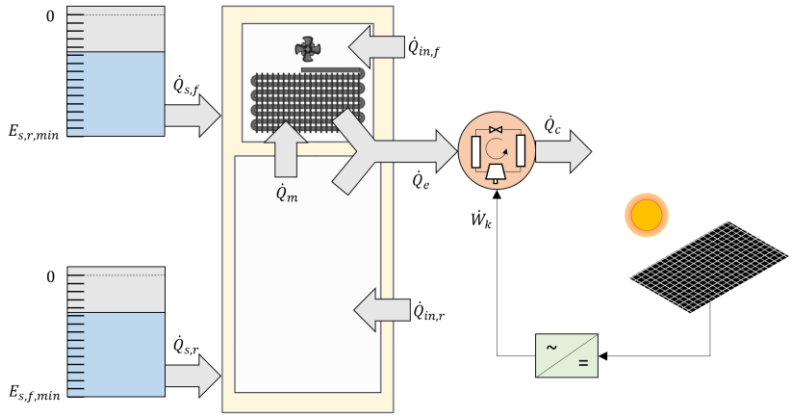

Figure 1: Schematic illustration of energy interactions during charge for a household refrigerator driven by photovoltaic power and with latent heat thermal energy storage.

2.1. Area of photovoltaic array

The PV array needs to be sized such that, for an interval of time under consideration, the total time that the refrigeration loop can operate at constant capacity is sufficient to remove the heat gained by the compartments during the time interval. Hence, it is necessary to estimate the relative duration of the charge and discharge modes. For a specific interval of time, Δt, a time integrated energy balance for the refrigerator is expressed as:

$$\left(\dot{Q}_{in,f,c}+\dot{Q}_{in,r,c}+\dot{W}_{v,f}+\dot{W}_{v,r}-\dot{Q}_e\right)\Delta t_c+\left(\dot{Q}_{in,f,d}+\dot{Q}_{in,r,d}\right)\Delta t_d=0 \tag{1}$$

Where the subscripts *f* and *r* are used for the frozen-food and fresh-food compartments, respectively, and the subscripts *c* and *d*, are used for the charge and discharge modes, respectively. In the energy balance presented in eq. (1), the LHTES units are considered to be inside the system boundaries. Hence, the heat transfer between the LHTES units and compartments, and across the mullion occurs internally to the thermodynamic system. From eq. (1), the required ratio, $r_{d,c}$, between the duration of discharge process and the duration of the charge process can be found as:

$$r_{d,c}=\frac{\Delta t_d}{\Delta t_c}=\frac{\dot{Q}_e-\dot{Q}_{in,f,c}-\dot{Q}_{in,r,c}-\dot{W}_{v,f}-\dot{W}_{v,r}}{\dot{Q}_{in,f,d}+\dot{Q}_{in,r,d}} \tag{2}$$

The duration of the charge process, Δt_c, and the duration of the discharge process, Δt_d, add up to the total interval of time Δt. Then, the compressor runtime ratio can be expressed as:

$$r_{on}=\Delta t_c/\Delta t=1/\left(1+r_{d,c}\right) \tag{3}$$

The power generated by the PV array depends on the solar irradiation, which varies with location and time. Assuming a constant total conversion efficiency for the PV subsystem, the power generated can be found as:

$$\dot{W}_{PV}\left(t\right)=\eta_{PV}A_{PV}I\left(t\right) \tag{4}$$

Where, η_{PV} is the total conversion efficiency for the PV subsystem, A_{PV} is the total solar collection, and I is the solar global irradiation on a horizontal surface. The system operates in charge mode when the PV power is sufficient to operate the refrigeration loop at constant capacity and drive the fans for air circulation. The power consumption of the refrigeration loop is related to the heat removal rate at the evaporator by means of the coefficient of performance (COP). Then, the required power input during charge is:

$$\dot{W}_{sys}=\dot{Q}_e/COP_R+\dot{W}_{v,f}+\dot{W}_{v,r} \tag{5}$$

The following function can be defined to mark the charge periods:

$$x_c\left(t\right)=\begin{cases}1 & if \quad \dot{W}_{PV}\left(t\right)\geq\dot{W}_{sys}\\ 0 & if \quad \dot{W}_{PV}\left(t\right)<\dot{W}_{sys}\end{cases} \tag{6}$$

Then, the area of the PV array needs to be chosen such that:

$$r_{d,c} = \frac{\Delta t_d}{\Delta t_c} = \frac{\int_{\Delta t} \left(1 - x_c(t)\right) dt}{\int_{\Delta t} x_c(t)\, dt} \tag{7}$$

In general, the irradiation profile cannot be expressed in a closed form. For a particular set of transient data, the area of the PV array needs to be determined numerically.

2.2. Discharge and charge power of LHTES units

For the stand-alone application under consideration, during discharge, the LHTES units keep the temperatures in the compartments in a range appropriate for food preservation without consuming electric power. To keep each compartment at near constant temperature, the LHTES unit must absorb heat at the same rate as the heat is being gained by the compartment. The required discharge power can be determined from an energy balance for the compartment considering the heat exchange with the LHTES unit as external.

$$\dot{Q}_{s.*,d} = \dot{Q}_{in,*,d} \pm UA_m \left(T_{r,d} - T_{f,d}\right) \tag{8}$$

Where the asterisk denotes the particular compartment, *f* for the frozen-food compartment and *r* for the fresh food compartment. The sign for the heat transfer rate across the mullion depends on the specific compartment; a positive sign is used for the frozen-food compartment while a negative sign is used for the fresh-food compartment.

To keep the compartment at a constant temperature during charge, the LHTES unit needs to dissipate heat at a rate that compensates the difference between the cooling rate and the compartment heat gain. The required discharge power can be determined from an instantaneous energy balance for the compartment considering the heat exchange with the LHTES unit as external.

$$\dot{Q}_{s.*,c} = \dot{Q}_{e,*} - \dot{Q}_{in,*,c} - \dot{W}_{v,*} \mp UA_m \left(T_{r,c} - T_{f,c}\right) \tag{9}$$

In eq. (9), the sign for the heat transfer rate across the mullion is negative for the frozen-food compartment and positive for the fresh-food compartment. The heat removal rate in each compartment can be expressed as a fraction of the total heat removal rate at the evaporator:

$$\begin{aligned} \dot{Q}_{e,f} &= f_{ref} \dot{Q}_e \\ \dot{Q}_{e,r} &= \left(1 - f_{ref}\right) \dot{Q}_e \end{aligned} \tag{10}$$

The refrigeration fraction, f_{ref}, can be found considering a time integrated energy balance for the frozen-food compartment, in which the heat exchange with the LHTES is regarded as internal. The refrigeration fraction is determined as:

$$f_{ref} = \left[r_{d,c} \left(\dot{Q}_{in,f,d} + UA_m \left(T_{r,d} - T_{f,d}\right) \right) + \dot{Q}_{in,f,c} + UA_m \left(T_{r,c} - T_{f,c}\right) + \dot{W}_{v,f} \right] \Big/ \dot{Q}_e \tag{11}$$

2.3. LHTES capacity

The LHTES capacity depends on the interval of time during which stand-alone operation of the system is required. During a particular interval of time, several periods of charge and discharge can occur, during which energy is removed and added to the LHTES. The energy change of the LHTES unit from the initial condition to a particular time can be found as:

$$\Delta E_{s,*}(t) = \int_0^t \left[\dot{Q}_{s,*,d} \left(1 - x_c\right) - \dot{Q}_{s,*,c} x_c \right] dt \tag{12}$$

During a specific interval of time, the energy change of the LHTES unit reaches a maximum and a minimum value. The required LHTES capacity is equal to the difference between the extreme values:

$$\Delta E_{s,*,\max} = \max\left(E_{s,*}(t)\right) - \min\left(E_{s,*}(t)\right) \tag{13}$$

3. DESIGN OF LHTES UNITS

3.1. Volume of phase change material

The LHTES units consist of panels filled with PCM materials that are located in the interior vertical walls of the compartments. The volume of PCM required in each compartment depends on the LHTES unit capacity, and is found as:

$$V_{PCM,*} = \Delta E_{s,*,\max} / \rho_{PCM,*} \lambda_{PCM,*} \tag{14}$$

3.2. Heat transfer considerations during discharge

The LHTES units are discharged by free convection to avoid any consumption of electric power during periods without solar energy availability. Free convection is driven by the temperature difference between the PCM and the air in the compartment, then, the heat transfer coefficients are restricted to low values. Hence, the use of extended surfaces is necessary to fulfill the discharge power requirements. The heat transfer design of the PCM panel is performed under the assumption that, during discharge, the free-convection resistance is much larger than the conduction resistance across the PCM. Heat transfer correlations for vertical fins are used (Bar-Cohen & Rohsenow, 1984) to define the geometric parameters of the finned surface that guarantee the discharge power. Rectangular straight fins are chosen because they are easy to manufacture. Figure 2(a) presents the geometric parameters of the LHTES units.

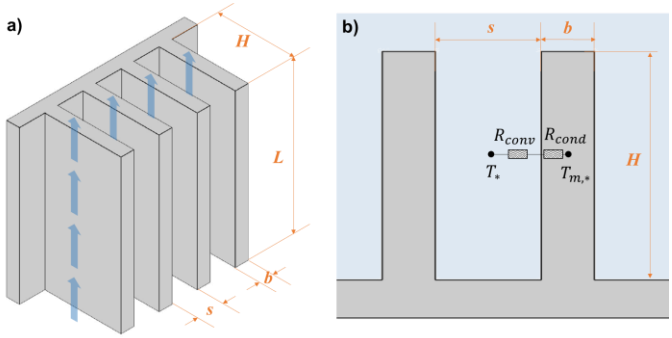

Figure 2: (a) Geometric parameters of finned surface design and (b) heat transfer model for the LHTES units.

The optimum spacing for thin fins at constant temperature is used (Bar-Cohen & Rohsenow, 1984):

$$s_{opt,*} = 2.714 L_* / Ra_{L,*} \tag{15}$$

Where the Rayleigh number, Ra_L, is based on the fin length, L. At the optimum spacing, the Nusselt number based on the fin spacing ($Nu_* = h_{s,*,d} s_{opt,*} / k_{air}$) has a value of 1.307. The discharge power of the LHTES unit can be expressed as:

$$Q_{s,d,*} = h_{s,*,d} \left(2 N_* H_* L_*\right)\left(T_{*,d} - T_{m,*}\right) \tag{16}$$

Considering that the base of the finned surface has negligible volume, the total volume of PCM in the LHTES unit can be expressed as:

$$V_{PCM,*} = N_* b_* H_* L_* \tag{17}$$

The finned PCM panels can be placed on all the vertical surfaces of each compartment excluding the door, which add to a total width of W_*. Then, the total number of fins, N_*, is restricted to be:

$$N_* = W_* / \left(s_* + b_*\right) \tag{18}$$

The fin length, H_*, fin width, b_*, and number of fins, N_*, are determined form equations (16), (17) and (18).

The bulk volume of the latent heat storage should be used in the assessment of the compartment capacity reduction because the space between the fins cannot be used for food storage. The fraction of the compartment volume occupied by the LHTES unit is found as:

$$f_{s,*} = H_* W_* L_* / V_* \tag{19}$$

The Biot number is used to compare the conduction resistance with the free-convection resistance, and to verify the assumption of negligible conduction resistance during discharge. The Biot number during discharge is defined as:

$$Bi_{*,d} = h_{s,*,d} b_* / 2 k_{PCM,*} \tag{20}$$

3.3. Heat transfer considerations during charge

To achieve the required charge power of the LHTES unit, the convection heat transfer coefficient needs to be enhanced by active circulation of air through the channels between the fins. Due to the increased convective transport, the conduction resistance can play a significant role during charge, and needs to be taken into account. Figure 2(b) illustrates the thermal resistance network applicable for the charge process. The charge power can be expressed as:

$$\dot{Q}_{s.*,c} = \frac{2N_* H_* L_*}{\left(\frac{1}{h_{s,*,c}} + \frac{b_*}{2k_{PCM,*}}\right)} \frac{\left(T_{o,*} - T_{m,*}\right) - \left(T_{*,d} - T_{m,*}\right)}{\ln\left(\frac{T_{o,*} - T_{m,*}}{T_{*,d} - T_{m,*}}\right)} \tag{21}$$

Steady flow is considered in each channel, and the conservation of energy equation can be expressed as:

$$\dot{Q}_{s,*,c} = N_* H_* s_* \rho_{air} v_{air} c_{p,air} \left(T_{o,*} - T_{*,d}\right) \tag{22}$$

An iterative procedure is used to determine the air velocity through the channels, $v_{air,*}$, the convective heat transfer coefficient, $h_{s,*,c}$, and the air temperature at the channel exit, $T_{o,*}$. Correlations for flow in a smooth duct are used for the heat transfer coefficient and the friction factor (Cengel, 2003). Interpolation is used for the transition regime between laminar and turbulent flow. The friction factor is used to obtain a first-order estimate of the dissipated power due to flow friction losses.

4. CASE DETAILS

4.1. Sample household refrigerator

The proposed design approach is demonstrated for a sample refrigerator that is representative of the preferences of the Colombian market and has the highest energy efficiency classification according to local regulations. The refrigerator is top-mount and frost-free, has a 105.6 L frozen-food compartment and a 294.1 L fresh-food compartment, and operates with R-600a. The thermal and geometric parameters of the sample refrigerator are summarized in Table 1. The compartment heat gains and the coefficient of performance for the refrigeration loop are estimated with the "Commercial Refrigerator Analysis" (CERA) software (UNIDO, 2013).

Table 1: Parameters for the sample household refrigerator

Compartment	**Frozen food**	**Fresh food**
Ambient temperature, T_a [°C]	32	
Temperature during LHTES discharge, $T_{*,d}$ [°C]	-18	5
Temperature during LHTES charge, $T_{*,c}$ [°C]	-22	1
Compressor power, $\dot{W}_k$ [W]	120	
Coefficient of performance, COP_R [-]	1.31	
Mullion thermal conductance, UA_m [W/K]	0.088	
Compartment heat gain during discharge, $\dot{Q}_{in,*,d}$ [W]	28.2	32.2
Compartment heat gain during charge, $\dot{Q}_{in,*,c}$ [W]	32.1	42.7
Power consumed for air circulation, $\dot{W}_{v,*}$ [W]	5	1.5
Compartment net capacity, V_* [L]	105.6	294.1
Length of vertical walls, L_* [m]	0.47	1.63
Total width of vertical walls, W_* [m]	1.36	1.63
Commercial PCM reference [a] [-]	PlusICE E-21	PlusICE A-2
PCM melting temperature, $T_{m,*}$ [°C]	-21	2
PCM latent heat capacity, $\lambda_{PCM,*}$ [kJ/kg]	285	230
PCM density, $\rho_{PCM,*}$ [kg/m^3]	1240	765
PCM thermal conductivity, $k_{PCM,*}$ [W/mK]	0.51	0.21

[a] Properties reported by (Phase Change Materials Products Limited, n.d.)

Commercial PCMs are selected for the frozen-food and fresh-food compartments (Phase Change Materials Products Limited, n.d.). A PCM with melting temperature of -21 °C is chosen for the frozen-food compartment and a PCM with a melting temperature 2 °C is chosen for the fresh-food compartment. The properties of the chosen PCMs are also listed in Table 1.The operating temperatures of the compartments and the melting temperatures of the PCMs are selected to have a temperature difference of 3 °C during discharge, and a temperature difference of 1 °C during charge. The higher temperature difference during the discharge enhances the free-convection heat transfer. Also, the temperature of the compartments needs to be kept in a narrow range to guarantee appropriate food storage conditions.

4.2. Solar energy availability

The assessment of the household refrigerator with LHTES and driven by PV power is performed using solar irradiation data for Medellín, Colombia. The weather in Medellín is warm year-round with a daily mean temperature of 22 °C. Medellín is close to Earth's equator and daylight time is around 12 h year-round. Data for thirty consecutive days with the lowest daily mean solar irradiation are taken from a typical meteorological year (European Comission, 2020), and used as the interval of time for the assessment. The daily mean solar irradiation on a horizontal surface is 5.16 kWh/m^2 for the complete typical meteorological year, and 4.04 kWh/m^2 for the selected data set. A total conversion efficiency of 15% is assumed for the PV subsystem.

5. RESULTS AND DISCUSSION

In this section, the results regarding system sizing and design of the LHTES units are discussed. The results are presented as a function of the compressor power because is a parameter that necessitates modification to operate the system solely with PV power. In general, runtime ratio for conventional refrigerators ranges between 0.40 and 0.50. Hence, the compressor capacity needs to be increased to reduce the runtime ratio and better accommodate to the solar energy availability profile.

5.1. Area of photovoltaic array and LHTES capacity

Figure 3(a) shows the behavior of the area of the PV array and the fraction of solar energy used with respect to compressor power. For the baseline value of 120 W for the compressor power, a large PV array of 17.5 m^2 is required. For this configuration, the runtime ratio is 0.44, and the compressor needs to run for most of the daylight hours. Hence, the area of the PV array needs to be large to generate enough PV power during periods of low solar irradiation. The oversized array leads to poor utilization of the PV electricity during periods of peak solar energy availability, and only 12% of the total PV electricity is effectively used. Initially, when the compressor power is increased, the area of the PV array drastically decreases while the fraction of solar electricity used quickly increases, because the power demand better matches the solar energy availability profile. For compressor power values greater than 140 W, the benefits of increasing the compressor power diminish, and the area of the PV array slowly approaches a value around 4.5 m^2. Similarly, the fraction of solar electricity used levels off at a modest value of 0.44. The use of a variable speed compressor could be considered to improve the utilization of solar electricity, and further reduce the area of the PV array.

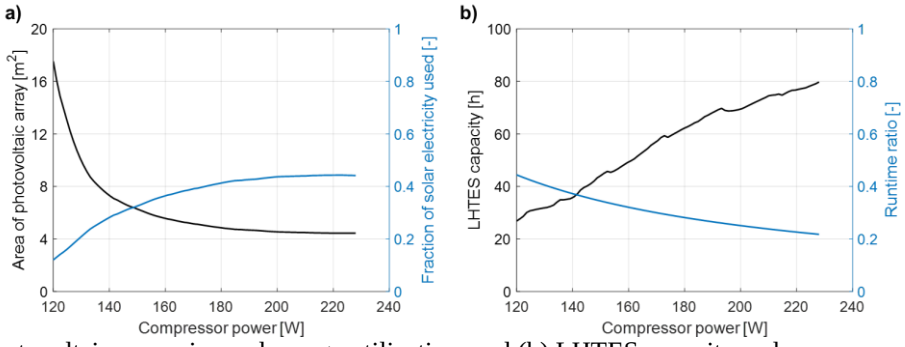

Figure 3: (a) photovoltaic array size and energy utilization, and (b) LHTES capacity and compressor runtime ratio.

Figure 3(b) presents the behavior of the LHTES capacity and the compressor runtime ratio as a function of the compressor power. The LHTES capacity increases almost linearly with the compressor power because the duration of the discharge period is increased. It is worth noting that, due to the daily variation in solar energy availability, LHTES capacities longer than 24 h may be required. During days of high solar energy availability, excess cooling capacity can be stored for later used during days of low solar energy availability. As observed in Figure 3(a) and

Figure 3(b) there is a trade-off between area of PV array and LHTES capacity. An economic analysis should be used to choose the compressor power that translates into the best configuration for these parameters.

5.2. Heat transfer design of LHTES units

The heat transfer restrictions imposed by the passive discharge of the LHTES dictate the geometry of the units in each compartment. Figure 4(a) shows the fraction of the compartment volume occupied by the LHTES units as a function of the compressor power. As can be seen in the figure, the LHTES units occupy a significant portion of each compartment. For the baseline value for the compressor power of 120 W, the LHTES units occupy 36 % of the fresh-food compartment and 41% of the frozen-food compartment. The volume occupied by the LHTES units slowly increases with compressor power, although the LHTES capacity strongly depends on compressor power. This behavior is explained by the dependence of the geometry of the LHTES units on the discharge power and the storage capacity. The required heat transfer area is the major factor in determining the geometry of the finned surface. The required heat transfer area is defined by the LHTES discharge power, which depends solely on the compartment heat gain and is independent of compressor power. The fin thickness and length are slightly affected by the quantity of PCM, which increases with the LHTES capacity. Hence, the geometry of the LHTES units weakly depends on compressor power. The volume occupied by the LHTES units could be reduced by improving the thermal insulation of the compartments, which would reduce the LHTES discharge power. In addition, and active and low-energy consumption approach could be considered to discharge the LHTES units. Figure 4(a) also shows the behavior of the Biot number during discharge. For the LHTES units in both compartments the Biot number remains below 0.1. Hence, the free-convection resistance dominates thermal transport during discharge, and the conduction resistance is negligible. During discharge, the low thermal conductivity of the PCMs does not hinder the performance of the LHTES.

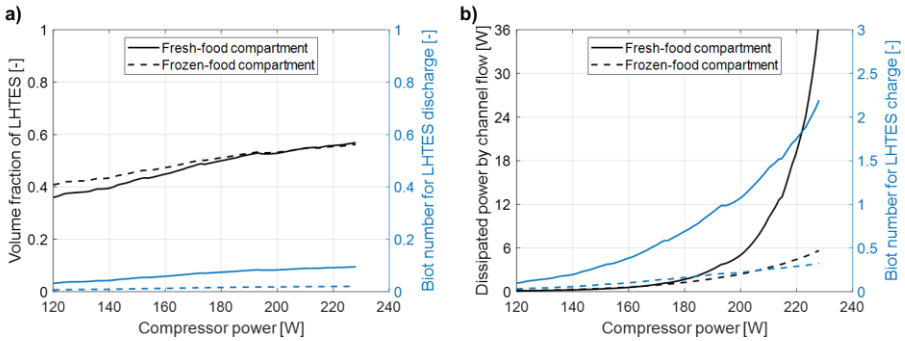

Figure 4: Design parameters for LHTES units associated to (a) the discharge process and (b) the charge process.

Figure 4(b) illustrates the heat transfer design considerations for the LHTES units during the charge process. Forced convection is required to achieve the required LHTES charge power. Hence, additional electric power needs to be spent to drive the air flow through the LHTES units. Figure 4(b) presents the behavior of the power dissipated due to flow friction. For compressor power values below 200 W, the flow friction losses are reasonable in both compartments. When the compressor power is further increased, the dissipated power due to flow friction increases rapidly to values that can significantly hinder the performance of the LHTES units, especially in the fresh-food compartment. The increase in dissipated power with compressor power is explained by the requirement of higher convection coefficients to respond to increments in fin thickness and charge power, both of which increase almost linearly with compressor power. During charge, conduction resistance across the PCM thickness can considerably affect heat transfer. As can be seen in Figure 4(b), the Biot number increases with compressor power. For the LHTES unit in the fresh-food compartment, conduction resistance becomes dominant when the compressor power is above 200 W (Bi > 1). In this compartment, the PCM has a lower thermal conductivity and a higher charge power is required.

6. CONCLUSIONS

The implemented thermal model is appropriate to establish design guidelines and assess the technical viability of a solar-driven household refrigerator with LHTES units. For the proposed case of study, it is concluded that, with moderate modifications, a commercial household refrigerator can operate in a stand-alone PV configuration using solely LHTES. However, the LHTES units occupy a considerable portion of the compartments volume due to the heat transfer restrictions imposed by the passive discharge. Some strategies could be implemented to significantly

reduced the volume the LHTES units such as: improving the thermal insulation of the compartments, actively discharging the LHTES units with a low-energy consuming approach, and widening the allowable temperature range for the compartments. Also, the systems sizing analysis indicates that the compressor power needs to be increased to reduce the required area for the PV array. However, there is a trade-off between the area of the PV array and the LHTES capacity, which increases linearly with compressor power. An economic analysis should be performed to establish the optimum configuration of the system.

NOMENCLATURE

A	photovoltaic	(m^2)
COP_R	coefficient of performance	(-)
b	fin thickness	(m)
Bi	Biot number	(-)
f	Fraction	(-)
E	energy	(kJ)
h	heat transfer coefficient	(W/m^2K)
H	fin depth	(m)
I	solar global irradiation	(W/m^2)
k	thermal conductivity	(W/mK)
L	fin length	(m)
Nu	Nusselt number	(-)
$\dot{Q}$	heat transfer rate	(W)
Ra	Rayleigh number	(-)
s	fin spacing	(m)
t	time	(s)
T	temperature	(°C)
UA	thermal conductance	(W/K)
V	volume	(m^3)
W	width of PCM panel	(m)
$\dot{W}$	power	(W)

Greek symbols

λ	latent heat	(kJ/kg)
ρ	density	(kg/m^3)
η	efficiency	(-)

Subscript

c	charge
d	discharge
e	evaporator
f	frozen food compartment
m	melting point
PCM	phase change material
PV	photovoltaic system
r	fresh food compartment
*	specific compartment (f or r)

REFERENCES

Bar-Cohen, A., & Rohsenow, W. W. (1984). Thermally optimum spacing of vertical, natural convection cooled, parallel plates. *Journal of Heat Transfer*, *106*(1), 116–123. https://doi.org/10.1115/1.3246622

Cengel, Y. A. (2003). *Heat transfer: A practical approach* (2nd Editio). Boston: McGraw-Hill.

El-Bahloul, A. A. M., Ali, A. H. H., & Ookawara, S. (2015). Performance and Sizing of Solar Driven dc Motor Vapor Compression Refrigerator with Thermal Storage in Hot Arid Remote Areas. *Energy Procedia*, *70*, 634–643. https://doi.org/10.1016/j.egypro.2015.02.171

European Comission. (2020). Joint Research Centre: Typical Meteorological Year. Retrieved from https://ec.europa.eu/jrc/en/PVGIS/tools/tmy

Ewert, M. K., Foster, R. E., & Estrada, L. (2001). Photovoltaic direct-drive, battery free solar refrigerator field test result. *ISES Solar World Congress*, (1).

Gin, B., Farid, M. M., & Bansal, P. K. (2010). Effect of door opening and defrost cycle on a freezer with phase change panels. *Energy Conversion and Management*, *51*(12), 2698–2706. https://doi.org/10.1016/j.enconman.2010.06.005

Gin, Benjamin, Farid, M. M., & Bansal, P. (2011). Modeling of phase change material implemented into cold storage application. *HVAC and R Research*, *17*(3), 257–267. https://doi.org/10.1080/10789669.2011.572222

Hasnain, S. M. (1998). Review on sustainable thermal energy storage technologies, Part II: cool thermal storage. *Energy Conversion and Management*, *39*(11), 1139–1153. Retrieved from http://linkinghub.elsevier.com/retrieve/pii/S0196890498000247

Khodadadi, J. M., Fan, L., & Babaei, H. (2013). Thermal conductivity enhancement of nanostructure-based colloidal suspensions utilized as phase change materials for thermal energy storage: A review. *Renewable and Sustainable Energy Reviews*, *24*, 418–444. https://doi.org/10.1016/j.rser.2013.03.031

Kibria, M. A., Anisur, M. R., Mahfuz, M. H., Saidur, R., & Metselaar, I. H. S. C. (2015). A review on thermophysical properties of nanoparticle dispersed phase change materials. *Energy Conversion and Management*, *95*, 69–89. https://doi.org/10.1016/j.enconman.2015.02.028

Kouassi, A. P. A., Touré, S., & Fassinou, W. F. (2020). Optimization of the production and storage of cold in a mechanical compression solar refrigerator. *African Journal of Science, Technology, Innovation and Development*, *12*(3), 305–316. https://doi.org/10.1080/20421338.2020.1755106

Mastani Joybari, M., Haghighat, F., Moffat, J., & Sra, P. (2015). Heat and cold storage using phase change materials in domestic refrigeration systems: The state-of-the-art review. *Energy and Buildings*, *106*, 111–124. https://doi.org/10.1016/j.enbuild.2015.06.016

Oró, E., de Gracia, A., Castell, A., Farid, M. M., & Cabeza, L. F. (2012). Review on phase change materials (PCMs) for cold thermal energy storage applications. *Applied Energy*, *99*, 513–533. https://doi.org/10.1016/j.apenergy.2012.03.058

Oró, Eduard, Miró, L., Farid, M. M., & Cabeza, L. F. (2012). Thermal analysis of a low temperature storage unit using phase change materials without refrigeration system. *International Journal of Refrigeration*, *35*(6), 1709–1714. https://doi.org/10.1016/j.ijrefrig.2012.05.004

Phase Change Materials Products Limited. (n.d.). PlusICE range. Retrieved from http://www.pcmproducts.net/Phase_Change_Material_Products.htm

Taneja, J., Lutz, K., & Culler, D. (2013). The impact of flexible loads in increasingly renewable grids. *2013 IEEE International Conference on Smart Grid Communications, SmartGridComm 2013*, 265–270. https://doi.org/10.1109/SmartGridComm.2013.6687968

Tarascon, J. M. (2010). Key challenges in future Li-battery research. *Philosophical Transactions of the Royal Society A: Mathematical, Physical and Engineering Sciences*, *368*(1923), 3227–3241. https://doi.org/10.1098/rsta.2010.0112

UNIDO. (2013). Commercial Refrigerator Analysis (CERA). United Nations Industrial Development Organization. Retrieved from https://github.com/unido/cera

ACKNOWLEDGEMENT

Authors would like to thank Universidad Pontificia Bolivariana and the alliance "ENERGETICA 2030", which is a Research Program, with code 58667 from the "Colombia Científica" initiative, funded by The World Bank through the call “778-2017 Scientific Ecosystems”. The research program is managed by the Colombian Ministry of Science, Technology and Innovation (MinCiencias) with contract No. FP44842-210-2018. Carolina Mira-Hernández also acknowledges financial support from MinCiencias and Universidad Pontificia Bolivariana through the call “848-2019 Postdoctoral Fellowships”.